AIP | The Journal of Chemical Physics

A multireference perturbation study of the NN stretching frequency of trans-azobenzene in nπ* excitation and an implication for the photoisomerization mechanism

Yu Harabuchi, Moe Ishii, Akira Nakayama, Takeshi Noro, and Tetsuya Taketsugu

Citation: J. Chem. Phys. **138**, 064305 (2013); doi: 10.1063/1.4790611
View online: http://dx.doi.org/10.1063/1.4790611
View Table of Contents: http://jcp.aip.org/resource/1/JCPSA6/v138/i6
Published by the American Institute of Physics.

A multireference perturbation study of the NN stretching frequency of *trans*-azobenzene in nπ^* excitation and an implication for the photoisomerization mechanism

Yu Harabuchi, Moe Ishii, Akira Nakayama, Takeshi Noro, and Tetsuya Taketsugu[a)]
Department of Chemistry, Faculty of Science, Hokkaido University, Sapporo 060-0810, Japan

(Received 13 October 2012; accepted 23 January 2013; published online 13 February 2013)

A multireference second-order perturbation theory is applied to calculate equilibrium structures and vibrational frequencies of *trans*-azobenzene in the ground and nπ^* excited states, as well as the reaction pathways for rotation and inversion mechanism in the nπ^* excited state. It is found that the NN stretching frequency exhibits a slight increase at the minimum energy structure in the nπ^* state, which is explained by the mixing of the NN stretching mode with the CN symmetric stretching mode. We also calculate the NN stretching frequency at several selected structures along the rotation and inversion pathways in the nπ^* state, and show that the frequency decreases gradually along the rotation pathway while it increases by ca. 300 cm^{-1} along the inversion pathway. The frequencies and energy variations along the respective pathways indicate that the rotation pathway is more consistent with the experimental observation of the NN stretching frequency in nπ^* excitation. © *2013 American Institute of Physics*. [http://dx.doi.org/10.1063/1.4790611]

I. INTRODUCTION

The photoisomerization of azobenzene has attracted a great deal of interests in both science and industry since the photoisomerization can be used as light-driven nanoscaled devices such as optical switches, and a great number of experimental studies have been reported.[1–18] An earlier study on the absorption spectra indicated that the first and second excited states of both *cis*- and *trans*-azobenzene were attributed to nπ^* and $\pi\pi^*$ excitations, respectively.[1,4,11] Quantum yields of the isomerizations for *cis*- and *trans*-azobenzene were reported to be different between nπ^* and $\pi\pi^*$ excitations.[1,2,4] Rau and Luddeke proposed that the photoisomerization of *trans*-azobenzene should follow different pathways in nπ^* and $\pi\pi^*$ excitations, through a comparison of the simple azobenzene and the sterically hindered azobenzenes.[5,7] It was reported that the nπ^* excitation invokes the inversion of the NNC bond angle within a planar geometry, while the $\pi\pi^*$ excitation invokes the rotation of two phenyl rings around the NN bond (Figure 1). Ultrafast UV-visible absorption spectroscopy and time resolved fluorescence experiments on *trans*-azobenzene suggested that decay in nπ^* excitation can be described by three processes:[1,2,4,9,11] (1) relaxation from the Franck-Condon region to the minimum in the $S_1(n\pi^*)$ state, (2) motion toward S_1/S_0 conical intersections, and (3) vibrational cooling in the S_0 state through an interaction with solvent molecules.

There have been several transient absorption experimental studies for the $\pi\pi^*$ excitation of *trans*- and *cis*-azobenzene.[8,11,13–15] Tahara and co-workers[12–14] carried out the time-resolved Raman, fluorescence, and absorption measurements with the $\pi\pi^*$ excitation of *trans*-azobenzene in solution. They clarified that isomerization proceeds in the nπ^* state after electronic relaxation, and proposed that the isomerization pathway is the same as that of direct nπ^* excitation. They also found that the NN stretching frequency shows only a slight decrease in the $S_1(n\pi^*)$ state.[12] Chang and co-workers examined the anisotropy of fluorescence of *trans*-azobenzene for nπ^* excitation in solution. They proposed that the photoisomerization proceeds through different pathways depending on the solution; the rotation pathway is taken in hexane while the concerted inversion pathway is preferred in ethylene glycol.[15]

There have been also a number of theoretical studies on the photoisomerization of azobenzene.[19–61] In an early study, Monti *et al.*[19] showed that in the $S_1(n\pi^*)$ state there is a large activation barrier along the rotation pathway while there is no barrier along the inversion pathway at the singly-excitation configuration interaction (CIS) level, indicating that the photoisomerization of *trans*- and *cis*-azobenzene is likely to proceed *via* the inversion pathway in nπ^* excitation. Monti *et al.* also suggested[19] that, in $\pi\pi^*$ excitation, the preferred pathway is a rotational route, which leads to either the photoisomerization *via* $S_1(n\pi^*)$ or no isomerization with direct transition to S_0.

In 1999, complete active space self-consistent field (CASSCF) method was employed to determine the rotation and inversion pathways between *trans*- and *cis*-azobenzene in the respective $S_1(n\pi^*)$ and $S_2(\pi\pi^*)$ states, in which the adiabatic potential energy was calculated with a multireference perturbation theory along the CASSCF reaction pathways. It was concluded that the inversion is probably the preferred pathway for nπ^* excitation while the rotation is preferred for $\pi\pi^*$ excitation.[22]

Ishikawa and co-workers[24] examined two-dimensional potential energy surfaces (PES) of the $S_1(n\pi^*)$ state as a function of the CNNC torsion and NNC bond angles at the multi-reference single and double excitation configuration

a)Author to whom correspondence should be addressed. Electronic mail: take@sci.hokudai.ac.jp. Fax: 81-11-706-4921.

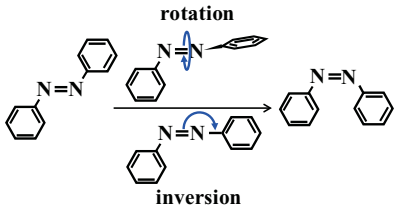

FIG. 1. A scheme of rotation and inversion mechanism for *cis-trans* isomerization of azobenzene.

interaction (MR-SDCI) level, and found an S_1/S_0 conical intersection along the rotation pathway, indicating that the rotation pathway is preferred in the $S_1(n\pi^*)$ state. After Ishikawa's report,[24] all theoretical studies at the CASSCF, multireference complete-active-space second-order perturbation theory (CASPT2), second-order approximated coupled-cluster model with the resolution-of-the-identity approximation (RI-CC2), and time-dependent density functional theory (TDDFT) levels indicate that the rotation is the preferred pathway for $n\pi^*$ excitation in the gas phase.[27,28,30,31,42,58]

On-the-fly dynamics simulations were also performed for the photoisomerization of azobenzene on the basis of semiempirical molecular orbital calculations with the surface hopping method[29,33,55,59,61] and with the multiple spawning method.[32] Recently, *ab initio* molecular dynamics (AIMD) simulations at the CASSCF level[26,47,54,57] and Car-Parrinello molecular dynamics simulations[34,45,49,50] were also performed for the photoisomerization of azobenzene in $n\pi^*$ excitation. In our surface hopping AIMD simulation[47] at the state-averaged CASSCF (SA-CASSCF) level, it was shown that *cis* to *trans* isomerization in $n\pi^*$ excitation occurs *via* two-step rotation mechanism, accompanying rotations of the central NN part and two phenyl rings, and this process can be classified into two types with respect to the orientation of the rotation, namely, clockwise and counterclockwise rotation pathways; the calculated quantum yields and lifetime in the excited states are in very good agreement with the corresponding experimental results.[47] The similar reaction mechanism was also reported in the dynamics simulations by Doltsinis *et al.*[45,49,50] and Thiel *et al.*[55]

As described above, the transient Raman spectra indicate that the NN stretching frequency of *trans*-azobenzene is almost unchanged (decreases by only 12 cm^{-1}) in the $S_1(n\pi^*)$ state.[12] There are several theoretical reports on vibrational frequencies for *trans*-azobenzene in the ground state at the MP2, density functional theory (DFT), and CASSCF levels,[20,21,23,25,30] while, to our knowledge, there is only one report on frequencies of *trans*-azobenzene in the $S_1(n\pi^*)$ state, which employed the CASSCF method.[30] However, the CASSCF method is sometimes insufficient for the quantitative discussion of geometries and frequencies because dynamical correlation effects are not taken into account.[62,63]

The goal of the current article has two-folds. One is to clarify the origin of small frequency shift in the NN stretching in the $n\pi^*$ state, and another is to show likely mechanism for *trans-cis* photoisomerization.

In order to gain insight to the photoisomerization mechanism of *trans*-azobenzene with reference to the Raman spectra, we employ the CASPT2 method to determine stationary points and vibrational frequencies for *trans*-azobenzene in both S_0 and $S_1(n\pi^*)$ states. This is the first attempt to discuss vibrational frequencies for the excited state of azobenzene by *ab initio* multireference theory.

II. COMPUTATIONAL DETAILS

Geometry optimizations and normal mode analyses were performed for *trans*-azobenzene in both S_0 and S_1 states under the C_{2h} symmetry restriction. In the S_0 state, DFT (B3LYP and CAM-B3LYP), Møller-Plesset second-order perturbation theory (MP2), quadratic configuration interaction with singles and doubles including triples perturbationally (QCISD(T)), SA-CASSCF, and CASPT2 methods were employed, while in the $S_1(n\pi^*)$ state TDDFT (B3LYP and CAM-B3LYP), SA-CASSCF, and CASPT2 methods were used. Normal mode analyses were also performed for an isotopomer of *trans*-azobenzene at optimized structures in both S_0 and S_1 states by substituting ^{14}N with ^{15}N to compare with the Raman spectra.[12] To examine the anharmonic effect, the direct vibrational self-consistent field (VSCF) and the following correlation-corrected VSCF (cc-VSCF) methods[64,65] were applied to both S_0 and S_1 states with quartic force field option[66] at the DFT(B3LYP)/6-31G* level.

In SA-CASSCF calculations, the S_0 and $S_1(n\pi^*)$ states are averaged with an equal weight, and the active space is chosen as 14 electrons in 12 orbitals (14,12), which includes two n orbitals and π/π^* orbitals of nitrogens, and four sets of π/π^* orbitals of phenyl rings. In CASPT2 calculations, the reference SA-CASSCF wavefunction is determined so that the active space includes two n orbitals and π/π^* orbitals of nitrogens ((6,4) active space); the lowest 17 orbitals are treated as frozen orbitals in the perturbation calculations for dynamic electron correlation. The active space of the reference CASSCF wavefunction for CASPT2 calculations was determined carefully to get the reliable results with available computational resources, through preliminary calculations; we verified that the equilibrium geometry in the ground state determined at the CASPT2 level with the CASSCF(6,4) reference is very similar to the equilibrium geometry determined at the CASPT2 level with the CASSCF(10,8) reference.[67]

We also investigated the *trans-cis* isomerization via the rotation pathway as a function of a CNNC torsion angle d_{CNNC} and the inversion pathway as a function of an NNC bond angle a_{NNC} on the $S_1(n\pi^*)$ PES. Optimization of the geometrical parameters was carried out by fixing d_{CNNC} to be 180° for the inversion pathway. Then, we calculated the NN stretching frequency along the respective pathways by applying a projection technique[68] at the CASPT2 level.

In the present calculations, Sapporo-DZP basis sets[69] were employed except for VSCF/cc-VSCF calculations. DFT calculations were performed by the GAMESS program package,[70] while MP2, CASPT2, and QCISD(T) calculations were performed by the MOLPRO2010 program package.[71]

III. RESULTS AND DISCUSSION

Table I shows calculated and experimental values for geometrical parameters and the NN stretching frequency at the

TABLE I. Geometrical parameters (bond length r in Å; bond angle a in degrees) and the harmonic frequency corresponding to the N-N stretching mode (ν_{NN} in cm^{-1}) in the ground state.

	r_{NN}	r_{CN}	a_{NNC}	ν_{NN}
DFT(B3LYP)	1.256	1.420	114.9	1556
DFT(CAM-B3LYP)	1.243	1.422	114.8	1637
MP2	1.279	1.426	113.3	1417
SA-CASSCF(14,12)	1.243	1.422	115.0	1694
CASPT2	1.265	1.432	113.3	1520
QCISD(T)	1.269	1.440	113.3	1522
Expt.	1.247[a]	1.428[a]	114.1[a]	1440[b]

[a]Reference 6.
[b]Reference 12.

TABLE II. Geometrical parameters (bond length r in Å; bond angle a in degrees) and the NN stretching harmonic frequency (ν_{NN} in cm^{-1}) for the C_{2h}-optimized structure in the $S_1(n\pi^*)$ state, as well as $n\pi^*$ vertical and adiabatic excitation energies (ΔE_{adi} and ΔE_{ver} in eV) within C_{2h} point group.

	r_{NN}	r_{CN}	a_{NNC}	ν_{NN}	ΔE_{adi}	ΔE_{ver}
TDDFT(B3LYP)	1.247	1.359	130.3	1672	1.95	2.55
TDDFT(CAM-B3LYP)	1.243	1.365	129.8	1727	2.20	2.76
SA-CASSCF(14,12)	1.252	1.367	128.5	1770	2.66	3.12
CASPT2	1.269	1.377	126.7	1581	2.39	2.87
Expt.	...	...	...	1428[a]	...	2.75[b]

[a]Reference 12.
[b]Reference 13.

equilibrium structure in the ground state of *trans*-azobenzene (referred to as $(S_0)_{min}$). The calculated geometrical parameters show good agreements with the experimental values so that the maximum differences are $\Delta r_{NN} \sim 0.032$ Å, $\Delta r_{CN} \sim 0.012$ Å, and $\Delta a_{NNC} \sim 0.9°$. The NN stretching frequency ν_{NN} is overestimated by ca. 80 cm^{-1} relative to the experimental fundamental frequency at the CASPT2 and QCISD(T) level, while it is underestimated by 23 cm^{-1} at the MP2 level. The cc-VSCF calculations at the DFT(B3LYP)/6–31G* level show that the harmonic and fundamental frequencies are 1561 and 1531 cm^{-1}, respectively, in the S_0 state, and thus the anharmonicity reduces the frequency by 30 cm^{-1}. By using this value in the other computational levels, a fundamental frequency for the NN stretching mode is estimated to be 1490 and 1492 cm^{-1} at the CASPT2 and QCISD(T) levels, respectively, which is comparable to the experimental value, 1440 cm^{-1}. There are several theoretical reports on equilibrium geometries and vibrational frequencies for *trans*-azobenzene in the ground state at the MP2, DFT, and CASSCF levels.[20,21,23,25,30] In an early study by Armstrong *et al.*,[20] r_{NN} and ν_{NN} were calculated to be 1.310 Å ($\Delta r_{NN} \sim 0.063$ Å) and 1296 cm^{-1}, respectively, at the MP2/6–31G level, while by replacing the basis set of nitrogen atoms with 6–31+G(d), r_{NN} and ν_{NN} were calculated to be 1.275 Å ($\Delta r_{NN} \sim 0.028$ Å) and 1450 cm^{-1}, respectively, so the addition of diffuse functions on nitrogen atoms improves the NN bond strength extensively.

For the $n\pi^*$ excited state, geometry optimization was performed under the C_{2h} symmetry constraint (the obtained structure is referred to as $(S_{1\text{-}C2h})_{min}$). Normal mode analyses indicate that $(S_{1\text{-}C2h})_{min}$ has one imaginary frequency mode, which corresponds to a torsional motion of the central -CNNC- (A_u symmetry) at DFT(CAM-B3LYP) ($20i$ cm^{-1}) and CASPT2 ($49i$ cm^{-1}) levels, while it has no imaginary frequency mode at the DFT(B3LYP) and SA-CASSCF levels. To examine instability of the planar geometry of *trans*-azobenzene in the $S_1(n\pi^*)$ state further, we performed additional DFT (B3LYP and CAM-B3LYP) and CASPT2 calculations using Sapporo-DZP plus diffuse functions, and found that the inclusion of diffuse functions does not change existence of the imaginary frequency mode. This result indicates that the planar structure of $(S_{1\text{-}C2h})_{min}$ is unstable with respect to the CNNC torsional motion, although an absolute value of these imaginary frequencies is not so large. We will come back to instability of the planar geometry later.

Table II shows geometrical parameters and the NN stretching frequency at $(S_{1\text{-}C2h})_{min}$, as well as $n\pi^*$ vertical and adiabatic excitation energies within the C_{2h} coordinate space. The calculated vertical excitation energy is in good agreement with the experimental value.[13] The comparison of geometrical parameters between S_0 and $S_1(n\pi^*)$ indicates that, by $n\pi^*$ excitation, the NN bond length is almost unchanged while the NNC bond angle increases by ca. 14° and the CN bond length decreases by ca. 0.06 Å. These geometrical changes can be explained by nature of molecular orbitals related to $n\pi^*$ excitation. Figure 2 shows natural orbitals relevant to $n\pi^*$ excitation, i.e., the lone pair n orbital of N atoms and the NN-π^* anti-bonding orbital, at the $(S_0)_{min}$ structure determined by the SA-CASSCF(6,4) calculations. As shown in Fig. 2, the n orbital shows anti-bonding nature for the NN bond, while the π^* orbital shows anti-bonding nature for the NN bond and bonding nature for two CN bonds; thus, due to $n\pi^*$ excitation, CN bonds should be strengthened while NN bond is not so affected. An increase in the NNC bond angle can be understood by noting the reduction of a repulsive force between bonding electron pairs (NN and CN bonds) and the lone pair of N atoms, which follows a valence shell electron pair repulsion (VSEPR) rule. A similar finding in geometrical changes of *trans*-azobenzene due to $n\pi^*$ excitation was also reported very recently at the semiempirical OM2/MRCI level.[61]

Experimentally, vibrational frequency was also measured for the isotopomer of *trans*-azobenzene (where ^{14}N is

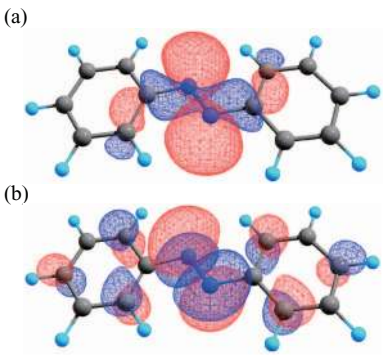

FIG. 2. Natural orbitals corresponding to (a) the lone pair orbital of nitrogen and (b) the NN anti-bonding π^* orbital of *trans*-azobenzene related to $n\pi^*$ excitation determined by the SA-CASSCF(6,4) calculation at $(S_0)_{min}$.

substituted by ^{15}N), and the isotopic shift in the NN stretching frequency was reported to be −27 and −29 cm^{-1} in the S_0 and S_1 states, respectively.[12] The corresponding isotopic shifts are calculated to be −31 and −37 cm^{-1} in the S_0 and S_1 states, respectively, at the DFT(B3LYP)/DZP level, which are in good agreement with the experimental values.[67] This agreement indicates that the experimentally observed frequency in the Raman spectra[12] is definitively ascribed to the NN stretching mode. As shown in Tables I and II, due to $n\pi^*$ excitation, the experimental NN stretching frequency decreases by 12 cm^{-1}, while the calculated frequency increases by 116 cm^{-1} (TDDFT(B3LYP)), 90 cm^{-1} (TDDFT(CAM-B3LYP)), 76 cm^{-1} (CASSCF), and 61 cm^{-1} (CASPT2). The anharmonicity effect in the NN stretching frequency is estimated to be 29 cm^{-1} (1679 → 1650 cm^{-1}) in the S_1 state as indicated by the cc-VSCF calculation at the TDDFT(B3LYP)/6-31G* level. The anharmonicity effect is similar to that in the ground state, and thus, change of the NN stretching fundamental frequency via $S_0 \rightarrow S_1$ excitation seems to be similar to the change of the harmonic one.

To our knowledge, there is one theoretical report on vibrational frequencies of *trans*-azobenzene in the $S_1(n\pi^*)$ state,[30] in which state-specific CASSCF calculations were performed to determine minimum energy structures and harmonic frequencies for the ground and $S_1(n\pi^*)$ states under the C_{2h} symmetry restriction, using the analytical gradient and analytical Hessian matrix, implemented in the MOLCAS-5.2 program.[72] The calculated frequencies, multiplied by scaling factor 0.91 to take into account effects of dynamic correlation and anharmonicity, were reported as 1440 cm^{-1} (S_0) and 1438 cm^{-1} (S_1), which were in good agreement with the experimental values. Since their results are totally different from our calculated values at the CASSCF/DZP level, we also performed geometry optimization and normal mode analyses by the same method, namely, the state-specific CASSCF with the (14,12) active space and the atomic natural orbital (ANO) basis sets, using the MOLCAS-6.4 program.[72] The calculated geometries and frequencies are almost identical to those in Ref. 30, and we have noticed, however, that the assignment for the NN stretching frequency at the CASSCF level in Ref. 30 is erroneous.[67] In our CASSCF calculations, the frequencies for the NN stretching mode are calculated to be 1701 cm^{-1} (S_0) and 1771 cm^{-1} (S_1), which are reduced to 1548 cm^{-1} and 1612 cm^{-1}, respectively, by applying the scaling factor of 0.91. This result is consistent with our CASSCF calculations with Sapporo-DZP basis sets, i.e., 1694 cm^{-1} (S_0) and 1770 cm^{-1} (S_1).

The increase in the NN stretching frequency due to $n\pi^*$ excitation can be understood by considering the mixing of normal modes.[73] As described above, $n\pi^*$ excitation strengthens both CN bonds, leading to an increase of force constants in the CN symmetric and anti-symmetric stretching modes. Then, an interaction between the CN symmetric stretching mode and the NN stretching mode of total symmetry representation results in the mixing of these two normal modes. Figure 3 shows the mechanism of the mixing of the NN stretching mode and the CN symmetric stretching mode due to $n\pi^*$ excitation. As shown in the figure, the NN stretching mode in the ground state shows almost a pure NN stretching motion while in the $S_1(n\pi^*)$ state, the corresponding mode contains a small contribution from a CN symmetric stretching motion; similarly, the original CN symmetric stretching mode contains a small contribution from NN stretching motion with anti-phase. As the result of this mixing, the frequency of the NN stretching mode increases from 1520 to 1581 cm^{-1}, while the frequency of the CN symmetric stretching mode decreases from 1235 to 1207 cm^{-1}.

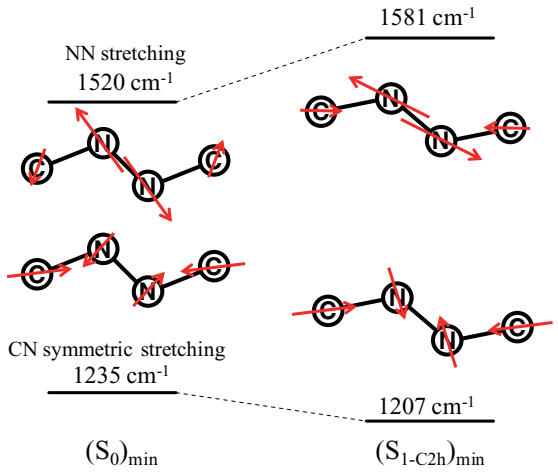

FIG. 3. A scheme of the mixing between the NN stretching mode and the CN symmetric stretching mode due to $n\pi^*$ excitation.

In order to examine the effect of CN symmetric stretching mode on the NN stretching frequency, we also performed geometry optimization and normal mode analyses for *trans*-diazene, N_2H_2, in the S_0 and $S_1(n\pi^*)$ states under the restriction of C_{2h} symmetry, by the CASPT2 method with Sapporo-DZP basis sets. The calculations show that, in N_2H_2, the π^* anti-bonding orbital is completely localized on the NN bond while the n orbital looks very similar to the one for *trans*-azobenzene in Fig. 2(a). Table III summarizes the calculated results. According to the present calculations, r_{NN}, r_{NH}, and a_{NNH} change as 1.265 → 1.290 Å, 1.045 → 1.026 Å, and 105.0 → 118.9°, respectively, and the NN stretching frequency changes as 1541 → 1478 cm^{-1}, due to $n\pi^*$ excitation, indicating that NN is weakened in the $S_1(n\pi^*)$ state. This result is consistent with chemical intuition, and therefore the origin of the increase in the NN stretching frequency of *trans*-azobenzene in the $S_1(n\pi^*)$ state can be ascribed to the mixing of the NN stretching mode and the CN symmetric stretching mode.

TABLE III. Geometrical parameters (bond length r in Å; bond angle a in degrees) of *trans*-diazene and harmonic frequencies for the NN stretching mode and the HNNH torsional mode (ν_{NN}, ν_{HNNH} in cm^{-1}) for C_{2h}-optimized structure in the S_0 and $S_1(n\pi^*)$ states, as well as $n\pi^*$ vertical and adiabatic excitation energies (ΔE_{ver} and ΔE_{adi} in eV) within C_{2h} point group at the CASPT2(12,10)/DZP level.

	r_{NN}	r_{NH}	a_{NNH}	ν_{NN}	ν_{HNNH}	ΔE_{ver}	ΔE_{adi}
S_0	1.265	1.045	105.0	1541	1308	3.38	...
$(S_{1\text{-}C2h})_{min}$	1.290	1.026	118.9	1478	621*i*	...	3.00

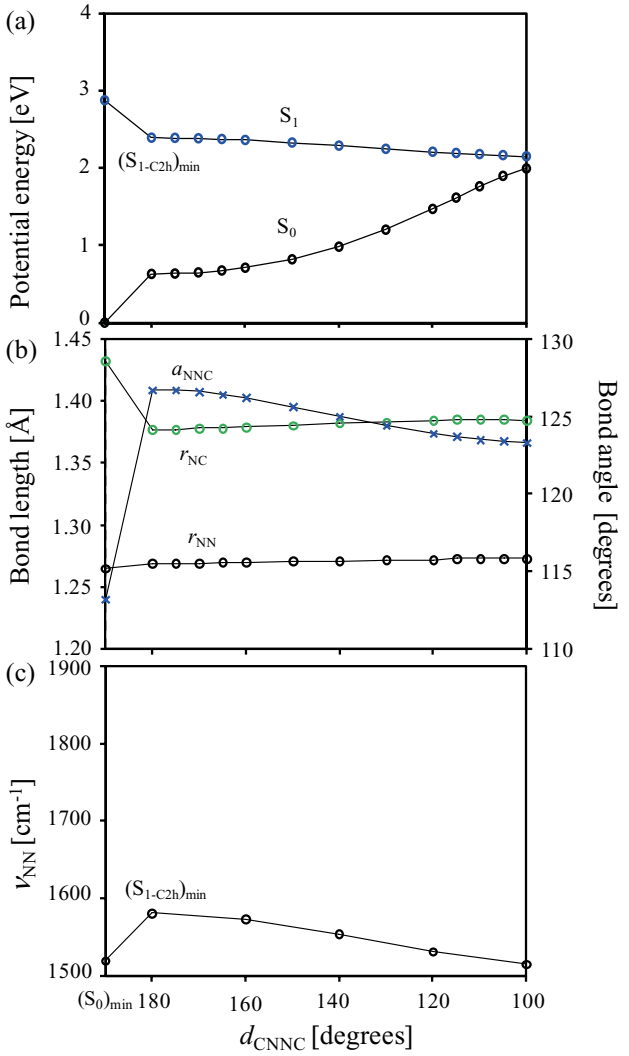

FIG. 4. Variations of (a) S_0 and S_1 energies, (b) important geometrical parameters, and (c) the NN stretching frequency along the rotation pathway.

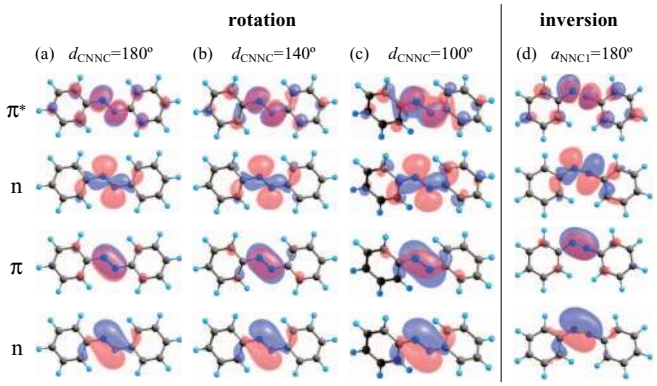

FIG. 5. A set of natural orbitals in the active space of SA-CASSCF(6,4) wavefunction at (a) $d_{CNNC} = 180^\circ$ ($(S_{1\text{-}C2h})_{min}$), (b) $d_{CNNC} = 140^\circ$, and (c) $d_{CNNC} = 100^\circ$, along the rotation pathway. The corresponding orbital set at $a_{NNC1} = 180^\circ$ on the inversion pathway is also given in (d).

As mentioned above, CASPT2 calculations show that the C_{2h} minimum of *trans*-azobenzene in the $S_1(n\pi^*)$ state has one imaginary frequency mode of A_u symmetry, which is directly related to a reaction coordinate of the rotation pathway, i.e., a torsion angle d_{CNNC}. To examine the feature of the reaction pathways from $(S_{1\text{-}C2h})_{min}$, we calculated the rotation pathway by choosing d_{CNNC} as a reaction coordinate and optimizing the other geometrical parameters by the CASPT2 method. Along the rotation pathway, vibrational frequencies were also calculated at the CASPT2 level with a projection technique[68] which gives a set of normal modes orthogonal to the rotation pathway by projecting out a component of the energy gradient in the Hessian matrix. Figure 4 shows variations of (a) S_0 and S_1 energies, (b) important geometrical parameters, and (c) the NN stretching frequency along the rotation pathway. Cartesian coordinates of geometries along the rotation pathway, as well as a variation of S_1 energies plus zero-point vibrational energies of transverse modes, are given in the supplementary material.[67] As shown in Fig. 4(a), the S_1-energy shows a gradual decrease until reaching a conical intersection of $(S_1/S_0)_{CI}$ around $d_{CNNC} \sim 95^\circ$. This result is consistent with a downhill feature of the rotation pathway derived from the semiempirical OM2/MRCI surface hopping simulations recently reported by Thiel *et al.*[61] It is very interesting to note that both r_{NN} and r_{CN} are almost unchanged along the rotation pathway as shown in Fig. 4(b). This result indicates that the NN bond order does not change while proceeding along the rotation pathway. Fig. 4(c) shows that the NN stretching frequency shows only a small decrease ($\sim$50 cm^{-1}) as d_{CNNC} changes from 180° to 100°; this small decrease is consistent with an almost constant bond length of the central NN bond.

From chemical intuition, the rotational motion about the central NN bond should weaken the NN bond because π-bonding orbital possibly breaks down. The calculated NN bond lengths and NN stretching frequencies, however, indicate that the NN bond is not weakened along the rotation pathway. To get insights to this mechanism, we examined variations of natural orbitals in the active space of SA-CASSCF(6,4) wavefunction. Figures 5(a)–5(c) show those natural orbitals in the active space determined at $d_{CNNC} = 180^\circ$, 140°, and 100°, respectively. As shown here, each orbital almost keeps its shape (i.e., n, π, n, π^*) while the molecule proceeds along the rotation pathway. The occupation numbers in these orbitals are also constant, $(n)^2(\pi)^2(n)^1(\pi^*)^1$ in the main configuration for different values of d_{CNNC}. No variation in the orbital shapes during the course of rotation is against chemical intuition, and this is the origin of the unchanged bond order of the central NN bond during the rotational motion.

We also calculated the inversion pathway by choosing a bond angle a_{NNC1} as a reaction coordinate where two carbon atoms of CNNC part are distinguished by C_1 and C_2, and optimizing other geometrical parameters by the CASPT2 method. Vibrational frequencies were also calculated along the inversion pathway at the same computational level. Figure 6 shows variations of (a) S_0 and S_1 energies, (b) important geometrical parameters, and (c) the NN stretching frequency along the inversion pathway; natural orbitals in the active space determined at $a_{NNC1} = 180^\circ$ are also shown in Figure 5(d). Cartesian coordinates of geometries along the inversion pathway, as well as a variation of S_1 energies plus zero-point vibrational energies of transverse modes, are given in the supplementary

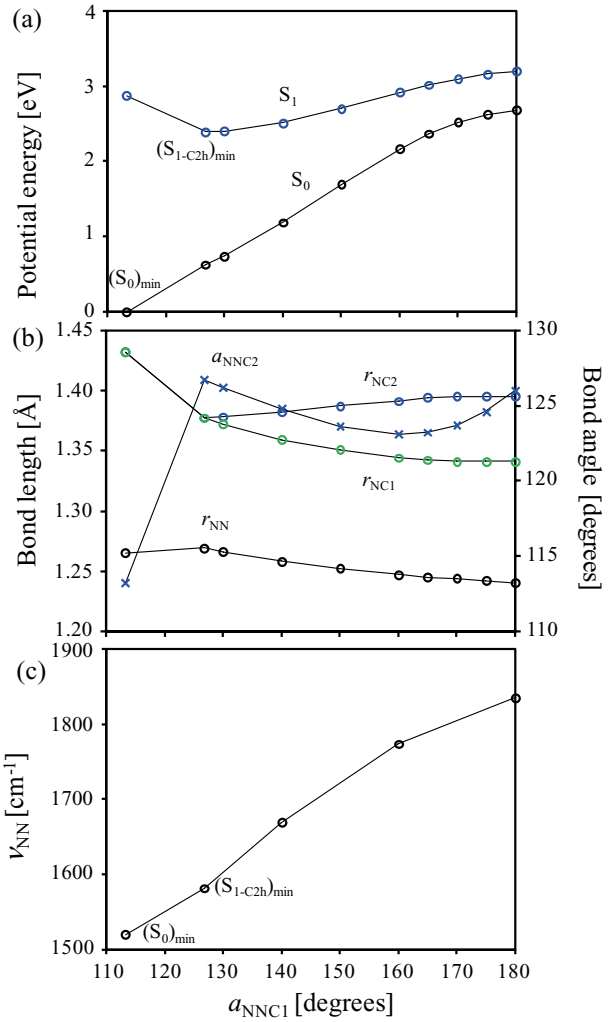

FIG. 6. Variations of (a) S_0 and S_1 energies, (b) important geometrical parameters, and (c) the NN stretching frequency along the inversion pathway.

material.[67] Along the inversion pathway, the S_1 energy shows an increase by ca. 0.8 eV at $a_{NNC} \sim 180^\circ$, and simultaneously the NN bond length decreases by 0.03 Å, and the NN stretching frequency increases by ca. 300 cm^{-1}. The increase of the NN bond order at $a_{NNC} \sim 180^\circ$ can be understood by noting that one of n orbitals gets π-bonding character as shown in Fig. 5(d). The increase in the adiabatic energy along the inversion pathway clearly indicates that *trans*-azobenzene prefers the rotation pathway, compared to the inversion pathway, in $n\pi^*$ excitation. This finding can explain, why in dynamics simulations the isomerization occurs through a rotation of the –N=N– fragment rather than a true torsion along the N–N bond.[47,55]

Finally, we summarize significant results from the present calculations. First, we should mention that we employ the CASPT2 method in determinations of geometrical structures, vibrational frequencies, and reaction pathways. Several studies employed *ab initio* multireference theory in the evaluations of the energy for geometries determined by the CASSCF method,[27,30,42] but to our best of knowledge, there has been no study to determine geometrical structures of stationary points and reaction pathways at the multireference correlated level. The energy variations along the reaction pathways clearly indicate that the rotation pathway is preferred to the inversion pathway. We also calculated the NN stretching frequencies for $(S_0)_{min}$, $(S_{1\text{-}C2h})_{min}$, and selected structures along the reaction pathways at the CASPT2 level, and compared those frequencies with the experimental values. A shift of the NN stretching frequency due to $n\pi^*$ excitation is relatively small, agreeing to the Raman spectra, although the frequency shows a decrease in the experiment while it shows an increase in the calculations.

IV. CONCLUDING REMARKS

In this work, we have examined the NN stretching frequency of *trans*-azobenzene in both S_0 and $S_1(n\pi^*)$ states thoroughly by *ab initio* multireference perturbation theory, CASPT2, to gain insights into the photoisomerization mechanism of *trans*-azobenzene. Through the time-resolved Raman measurements in solution, Tahara *et al*. found that the NN stretching frequency shows only a slight decrease in the $S_1(n\pi^*)$ state.[12] Our CASPT2 calculations show that, due to $n\pi^*$ excitation, the NN bond length changes little (~0.004 Å) and the NN stretching frequency increases only by 64 cm^{-1} at the C_{2h} minimum on the S_1-PES; the former is explained in terms of molecular orbitals related to $n\pi^*$ excitation while the latter is explained by the mixing of the NN stretching normal mode with the CN symmetric stretching normal mode.

It is also shown that the C_{2h} minimum of *trans*-azobenzene in the $S_1(n\pi^*)$ state is unstable with respect to the CNNC torsion angle, although an absolute value of the imaginary frequency of the related mode is not large. We also calculated the rotation and inversion pathways as a function of d_{CNNC} and a_{NNC}, respectively, at the CASPT2 level, and then calculated the NN stretching frequency along the respective reaction pathways by a projection technique. The calculated NN stretching frequency shows a slight decrease along the rotation pathway while it increases rapidly along the inversion pathway. The almost constant bond order of the central NN bond along the rotation pathway is explained in terms of little changes of orbital shapes. A small variation of the NN stretching frequency along the rotation pathway suggests the possibility that in the experimental Raman spectra,[12] vibrational motion of the molecule under structural transformation along the rotation pathway is observed, and our CASPT2 calculations support the rotation pathway as a preferred one in the $n\pi^*$ excitation of *trans*-azobenzene.

Finally, it should be noted that our calculations support the rotation mechanism in the gas phase, and there remains a possibility of other reaction mechanism in solution, depending on the type of solvent molecules.

ACKNOWLEDGMENTS

We are sincerely grateful to Professor Tahei Tahara (RIKEN) and Professor Nikita Matsunaga (Long Island University) for valuable discussions and providing valuable comments on our manuscript. We also thank Mr. Kiminori Satoh for his contribution in the initial stage of the present

study. This work was supported by a Grant-in-Aid for Scientific Research from the Ministry of Education, Culture, Sports, Science and Technology. The computations were performed using the Research Center for Computational Science, Okazaki, Japan. Y.H. thanks a support from the Japan Society for the Promotion of Science for Research Fellowships for Young Scientist.

[1]G. Zimmerman, L.-Y. Chow, and U.-J. Paik, J. Am. Chem. Soc. **80**, 3528 (1958).
[2]D. Gegiou, K. A. Muszkat, and E. Fisher, J. Am. Chem. Soc. **90**, 12 (1968).
[3]A. Mostad and C. Romming, Acta Chem. Scand. **25**, 3561 (1971).
[4]P. Bortolus and S. Monti, J. Phys. Chem. **83**, 648 (1979).
[5]H. Rau and E. Luddeke, J. Am. Chem. Soc. **104**, 1616 (1982).
[6]J. A. Bouwstra, A. Schouten, and J. Kroon, Acta Crystallogr., Sect. C: Cryst. Struct. Commun. **39**, 1121 (1983).
[7]H. Rau, in *Photochromism: Molecules and Systems*, edited by H. Durr and H. Bounas-Laurent (Elsevier, Amsterdam, 1990), Vol. 1, Chap. 4, pp. 165–192.
[8]I. K. Lednev, T.-Q. Ye, R. E. Hester, and J. N. Moore, J. Phys. Chem. **100**, 13338 (1996).
[9]T. Nagele, R. Hoche, W. Zinth, and J. Wachtveitl, Chem. Phys. Lett. **272**, 489 (1997).
[10]N. Biswas and S. Umapathy, J. Chem. Phys. **107**, 7849 (1997).
[11]I. K. Lednev, T.-Q. Ye, P. Matousek, M. Towrie, P. Foggi, F. V. R. Neuwahl, S. Umapathy, R. E. Hester, and J. N. Moore, Chem. Phys. Lett. **290**, 68 (1998).
[12]T. Fujino and T. Tahara, J. Phys. Chem. A **104**, 4203 (2000).
[13]T. Fujino, S. Y. Arzhantsev, and T. Tahara, J. Phys. Chem. A **105**, 8123 (2001).
[14]T. Fujino, S. Y. Arzhantsev, and T. Tahara, Bull. Chem. Soc. Jpn. **75**, 1031 (2002).
[15]C.-W. Chang, Y.-C. Lu, T.-T. Wang, and E. W.-G. Diau, J. Am. Chem. Soc. **126**, 10109 (2004).
[16]C. M. Stuart, R. R. Frontiera, and R. A. Mathies, J. Phys. Chem. A **111**, 12072 (2007).
[17]J. Bao and P. M. Weber, J. Am. Chem. Soc. **133**, 4164 (2011).
[18]Z. Dong, N. M. Seemann, N. Lu, and Y. Song, J. Phys. Chem. B **115**, 14912 (2011).
[19]S. Monti, G. Orlandi, and P. Palmieri, Chem. Phys. **71**, 87 (1982).
[20]D. R. Armstrong, J. Clarkson, and W. E. Smith, J. Phys. Chem. **99**, 17825 (1995).
[21]N. Biswas and S. Umapathy, J. Phys. Chem. A **101**, 5555 (1997).
[22]P. Cattaneo and M. Persico, Phys. Chem. Chem. Phys. **1**, 4739 (1999).
[23]N. Kurita, S. Tanaka, and S. Itoh, J. Phys. Chem. A **104**, 8114 (2000).
[24]T. Ishikawa, T. Noro, and T. Shoda, J. Chem. Phys. **115**, 7503 (2001).
[25]H. Fliegl, A. Kohn, C. Hattig, and R. Ahlrichs, J. Am. Chem. Soc. **125**, 9821 (2003).
[26]T. Schultz, J. Quenneville, B. Levine, A. Toniolo, T. J. Martinez, S. Lochbrunner, M. Schmitt, J. P. Shaffer, M. Z. Zgierski, and A. Stolow, J. Am. Chem. Soc. **125**, 8098 (2003).
[27]A. Cembran, F. Bernardi, M. Garavelli, L. Gagliardi, and G. Orlandi, J. Am. Chem. Soc. **126**, 3234 (2004).
[28]E. W.-G. Diau, J. Phys. Chem. A **108**, 950 (2004).
[29]C. Ciminelli, G. Granucci, and M. Persico, Chem.-Eur. J. **10**, 2327 (2004).
[30]L. Gagliardi, G. Orlandi, F. Bernardi, A. Cembran, and M. Garavelli, Theor. Chem. Acc. **111**, 363 (2004).
[31]M. L. Tiago, S. Ismail-Beigi, and S. G. Louie, J. Chem. Phys. **122**, 094311 (2005).
[32]A. Toniolo, C. Ciminelli, M. Persico, and T. J. Martinez, J. Chem. Phys. **123**, 234308 (2005).
[33]C. Ciminelli, G. Granucci, and M. Persico, J. Chem. Phys. **123**, 174317 (2005).
[34]C. Nonnenberg, H. Gaub, and I. Frank, Chem. Phys. Chem. **7**, 1455 (2006).
[35]G. Fuechsel, T. Klamroth, J. Dokic, and P. Saalfrank, J. Phys. Chem. B **110**, 16337 (2006).
[36]C. R. Crecca and A. E. Roitberg, J. Phys. Chem. A **110**, 8188 (2006).
[37]L. Briquet, D. P. Vercauteren, E. A. Perpète, and D. Jacquemin, Chem. Phys. Lett. **417**, 190 (2006).
[38]G. Granucci and M. Persico, Theor. Chem. Acc. **117**, 1131 (2007).
[39]I. Conti, F. Marchioni, A. Credi, G. Orlandi, G. Rosini, and M. Garavelli, J. Am. Chem. Soc. **129**, 3198 (2007).
[40]S. Yuan, Y. Dou, W. Wu, Y. Hu, and J. Zhao, J. Phys. Chem. A **112**, 13326 (2008).
[41]J. Shao, Y. Lei, Z. Wen, Y. Dou, and Z. Wang, J. Chem. Phys. **129**, 164111 (2008).
[42]I. Conti, M. Garavelli, and G. Orlandi, J. Am. Chem. Soc. **130**, 5216 (2008).
[43]P. Sauer and R. E. Allen, Chem. Phys. Lett. **450**, 192 (2008).
[44]T. Cusati, G. Granucci, M. Persico, and G. Spighi, J. Chem. Phys. **128**, 194312 (2008).
[45]M. Böckmann, N. L. Doltsinis, and D. Marx, Phys. Rev. E **78**, 036101 (2008).
[46]P. Sauer and R. E. Allen, J. Phys. Chem. A **112**, 11142 (2008).
[47]Y. Ootani, K. Satoh, A. Nakayama, T. Noro, and T. Taketsugu, J. Chem. Phys. **131**, 194306 (2009).
[48]L. Wang, W. Xu, C. Yi, and X. Wang, J. Mol. Graphics Modell. **27**, 792 (2009).
[49]M. Böckmann, N. L. Doltsinis, and D. Marx, Angew. Chem. **122**, 3454 (2010).
[50]M. Böckmann, N. L. Doltsinis, and D. Marx, J. Phys. Chem. A **114**, 745 (2010).
[51]L. De Boni, C. Toro, S. C. Zilio, C. R. Mendonca, and F. E. Hernandez, Chem. Phys. Lett. **487**, 226 (2010).
[52]M. Dubecký, R. Derian, L. Mitas, and I. Štich, J. Chem. Phys. **133**, 244301 (2010).
[53]C.-W. Jiang, R.-H. Xie, F.-L. Li, and R. E. Allen, J. Phys. Chem. A **115**, 244 (2011).
[54]T. Cusati, G. Granucci, and M. Persico, J. Am. Chem. Soc. **133**, 5109 (2011).
[55]O. Weingart, Z. Lan, A. Koslowski, and W. Thiel, J. Phys. Chem. Lett. **2**, 1506 (2011).
[56]M. Dubecky, R. Derian, L. Horvathova, M. Allan, and I. Stich, Phys. Chem. Chem. Phys. **13**, 20939 (2011).
[57]M. Pederzoli, J. Pittner, M. Barbatti, and H. Lischka, J. Phys. Chem. A **115**, 11136 (2011).
[58]R. J. Maurer and K. Reuter, J. Chem. Phys. **135**, 224303 (2011).
[59]T. Cusati, G. Granucci, E. Martínez-Núñez, F. Martini, M. Persico, and S. Vázquez, J. Phys. Chem. A **116**, 98 (2012).
[60]H. M. D. Bandara and S. C. Burdette, Chem. Soc. Rev. **41**, 1809 (2012).
[61]J. A. Gamez, O. Weingart, A. Koslowski, and W. Thiel, J. Chem. Theory Comput. **8**, 2352 (2012).
[62]X.-F. Yu, S. Yamazaki, and T. Taketsugu, J. Chem. Theory Comput. **7**, 1006 (2011).
[63]S. Yamazaki and T. Taketsugu, J. Phys. Chem. A **116**, 491 (2012).
[64]G. M. Chaban, J. O. Jung, and R. B. Gerber, J. Chem. Phys. **111**, 1823 (1999).
[65]K. Yagi, T. Taketsugu, K. Hirao, and M. S. Gordon, J. Chem. Phys. **113**, 1005 (2000).
[66]K. Yagi, K. Hirao, T. Taketsugu, M. W. Schmidt, and M. S. Gordon, J. Chem. Phys. **121**, 1383 (2004).
[67]See Supplementary Material at http://dx.doi.org/10.1063/1.4790611 for Cartesian coordinates and vibrational frequencies of stationary points, Cartesian coordinates of selected points along the reaction pathways, and variations of adiabatic potential energies plus zero-point vibrational energies of normal modes orthogonal to the reaction pathways.
[68]W. H. Miller, N. C. Handy, and J. E. Adams, J. Chem. Phys. **72**, 99 (1980).
[69]T. Noro, M. Sekiya, and T. Koga, Theo. Chem. Acc. **131**, 1124 (2012).
[70]M. W. Schmidt, K. K. Baldridge, J. A. Boatz, S. T. Elbert, M. S. Gordon, J. H. Jensen, S. Koseki, N. Matsunaga, K. A. Nguyen, S. J. Su, T. L. Windus, M. Dupuis, and J. A. Montgomery, J. Comput. Chem. **14**, 1347 (1993).
[71]MOLPRO, version 2010.1, a package of *ab initio* programs, H.-J. Werner, P. J. Knowles, G. Knizia, F. R. Manby, M. Schutz *et al.*, see http://www.molpro.net.
[72]G. Karlström, R. Lindh, P.-Å. Malmqvist, B. O. Roos, U. Ryde, V. Veryazov, P.-O. Widmark, M. Cossi, B. Schimmelpfennig, P. Neogrady, and L. Seijo, Comput. Mater. Sci. **28**, 222 (2003).
[73]T. Hirano, T. Taketsugu, and Y. Kurita, J. Phys. Chem. **98**, 6936 (1994).